HiSST: 3rd International Conference on
High-Speed Vehicle Science Technology
14 -19 April 2024, Busan, Korea

Sizing Optimization of Fixed Cross-Section of Combustor in Ramjet Engine for Hypersonic Transport Considering Trajectory

Yingchen Liu[1], Feng Guo[2], Jianfeng Zhu[3], and Yancheng You[4]

Abstract

Based on the Gauss pseudospectral trajectory optimization method, a methodology for aircraft/engine integration of ramjet engine was established. Focusing on ramjet engines operating within a wide speed range (Mach 2.5 - Mach 5), considering the characteristics of aircraft lift-to-drag ratio and flight trajectory, the sizing optimization of fixed cross-section of combustor in ramjet engine was accomplished with the objective of minimizing fuel consumption in the climb phase. The research findings indicate that: An optimal value exists for the cross-sectional size of the ramjet combustor that minimizes fuel consumption during the climb phase. Under the optimal trajectory, with the combustor area at 5.2 m^2, fuel consumption is reduced by 208 kg (7.1%) compared to 4 m^2 and 200 kg (6.8%) compared to 6 m^2.

Keywords: *ramjet engine; gauss pseudospectral method; optimization; hypersonic; matching design*

Nomenclature

h – Altitude
V – Velocity
γ – Climbing angle
T – Thrust
α – Attack angle
D – Drag, Diameter
m – Aircraft weight
C_L – Lift coefficient
C_D – Drag coefficient
r – Trajectory radius
q – Dynamic pressure
S – Wing area
σ – Recovery coefficient
φ – Capture coefficient
C – Coefficient
M – Mach number
$L_{in,r}$ –central cone relative length
$L_{in,cr}$ – central cone relative length in critical state
θ, δ – Position angle
λ – velocity coefficients
k – specific heat ratio
η – efficiency
P – Pressure
f – fuel-air ratio
τ – temperature rise ratio
C_{Fe} –Thrust coefficient
W – Mass flow
β – expansion angle
Isp – Specific impulse

Superscripts
· – Derivative
* – total

Subscripts
max – maximum
x – Spillage drag
shock – shock wave
b – capture
ch – cone
c – cone, combustor
ad – addition
s – Separation
a – air
f – fuel, final

[1] *School of Aerospace Engineering, Xiamen University, China, abcde@stu.xmu.edu.cn*
[2] *School of Aerospace Engineering, Xiamen University, China, 2021175150@xmu.edu.cn*
[3] *School of Aerospace Engineering, Xiamen University, China, zhjf@xmu.edu.cn*
[4] *School of Aerospace Engineering, Xiamen University, China, yancheng.you@xmu.edu.cn*

1. Introduction

Hypersonic aircraft, renowned for their exceptional penetration capabilities and rapid striking potential, have garnered significant attention in global research [1-2]. Traditionally, hypersonic aircraft have relied on mature rocket engine technology for propulsion. However, inherent limitations within rocket engines, typically characterized by specific impulse values of around 300 seconds, present minimal scope for enhancement. In pursuit of achieving hypersonic flight with elevated specific impulse, ramjet engines have emerged as a promising alternative [3]. The evolution of ramjet engine technology has been marked by rapid advancement over the past century. Owing to their comparatively simpler structural design compared to turbojet engines, coupled with superior specific impulse and fuel efficiency within the Mach 2 to Mach 5 regime [4], ramjet engines have found widespread utilization within hypersonic flight research domains [5].

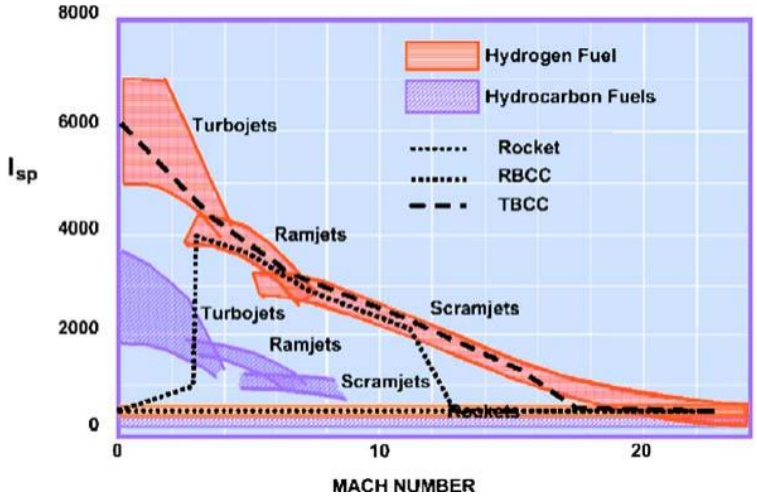

Fig 1. Air breathing hypersonic propulsion cycles provide enhanced propulsion efficiency [6]

As the Fig 2 shows, the ramjet engine comprises main components including the inlet, combustor, and nozzle. Depending on the Mach number of the inlet airflow into the combustor, ramjet engines are categorized into various types such as ramjet engines, scramjet engines, dual-mode scramjet engines, and dual-combustor scramjet engines. During operation, the ramjet engine functions by compressing high-speed incoming airflow through the inlet, the air enters the combustor with the highest possible total pressure recovery coefficient. Within the combustor, the air mixes with fuel and undergoes combustion. Subsequently, the high-temperature gas at subsonic speeds expands within the nozzle and is expelled at high velocity, thereby generating thrust [7]. As the flight Mach number increases, the total temperature and pressure of the airflow experience a significant rise. However, if the incoming flow is further decelerated to subsonic speeds, the static temperature of the airflow might surpass the temperature limit of the combustor material. This scheme can induce intense fuel thermal decomposition, absorbing a substantial amount of heat energy and resulting in reduced combustion energy release efficiency and poor engine performance. Therefore, the flight Mach number range suitable for ramjet engines is typically around 2.5 to 5.

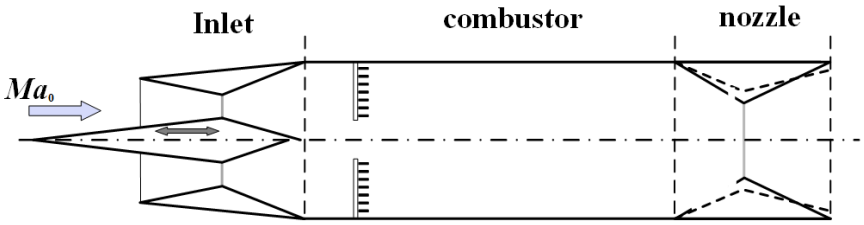

Fig 2. Schematic diagram of ramjet engine

Ramjet engines typically select the cruising state as the design point. However, since ramjet engines have a wide operating range, the performance of the engine at off-design points cannot be overlooked. When the engine is operating at a off-design point, the airflow captured by the inlet may deviate from optimal levels, either being too low or too high. This deviation can lead to a reduction in engine thrust

or an increase in spillage drag, consequently undermining engine performance. To effectively navigate complex operational schemes, it's essential to comprehensively consider the engine's performance across a wide speed range and reasonably design the engine. For short-range aircraft operating within flight Mach numbers ranging from 3 to 4, the acceleration process tends to be relatively brief, with less emphasis placed on off-design point conditions. However, in the case of hypersonic aircraft, the significant drag results in diminished net thrust, and the duration of the climb phase gradually approaches that of the cruising process. As a result, there is a need to weaken the design point, ensuring optimization of the aircraft/engine system across the whole flight process. Such an approach is indispensable for achieving optimal performance and efficiency throughout the design phase.

To enhance the performance of aircraft/engine systems, optimization is essential across various aspects, including structure, design, and control. As flight speeds increase, the unique structural design of air-breathing aircraft intensifies the interaction between subsystems, particularly the coupling between the aircraft and the engine. Consequently, research involving aerodynamic heating, flow combustion, system control, and other related issues becomes more intricate. Therefore, research on aircraft/engine system integration serves as the theoretical foundation and technological backbone for the study and development of hypersonic propulsion technology. It holds significant theoretical value and engineering significance.

This study focuses on the design of a ramjet engine for a particular hypersonic transport aircraft, intended for both climb missions within the Mach 2.5 to Mach 5 speed range. trajectory optimization of the aircraft is used to assist in designing the optimal size of the combustor cross-section of the ramjet engine. The purpose of this study is to improve the propulsion efficiency of the aircraft during the climb phase while simultaneously extending the range of the hypersonic transport.

2. Problem statement

Ramjets propel the aircraft during the climb phase and then operate during the long-distance and high-speed (Mach 5+) cruise phase. It is noteworthy that the range is one of the most crucial indicators for evaluating the overall performance of hypersonic transport. For low-speed aircraft, the cruise phase holds greater significance than the climb phase because it contributes significantly more to the overall range. However, in the case of hypersonic transport, the fuel consumption during the climb phase cannot be ignored. For hypersonic transport, fuel consumption during the climb phase increases dramatically, thus reducing both the vehicle's initial weight and the available fuel at the start of the cruise phase.

Ramjets designed with a single-design-point pattern typically exhibit good performance, yet their efficiency falters under varying operating conditions. The most significant reason causing this issue is that the fixed geometrical dimensions of certain ramjet components, such as the cross-sectional area (A3) of the combustion chamber. When the cross-sectional area A3 is either too large or too small, it becomes challenging to achieve proper combustion or results in excessive windward resistance, thereby hindering the engine from achieving optimal performance in both lower and higher Mach flight conditions. Consequently, the cross-sectional area A3 significantly influences the overall performance of a aircraft during the wide-Mach number climb phase. Fig 3 illustrates the required thrust and the corresponding A3 values of the ramjet design at each flight point condition along the trajectory of constant dynamic pressure from Mach 2.5 to 5. Under conditions of constant acceleration, the A3 of the designed ramjet varies with the flight Mach number. When A3 remains fixed, the captured mass flow rate exceeds the combustor's requirements, resulting in excess air overflow and increased drag during low-Mach number conditions. Correspondingly, designing the ramjet with a larger A3 can resolve the overflow issue at low speeds, but it results in increased resistance at high speeds due to the engine's larger size. Consequently, this would result in diminished performance of the aircraft during the high-Mach number cruise phase.

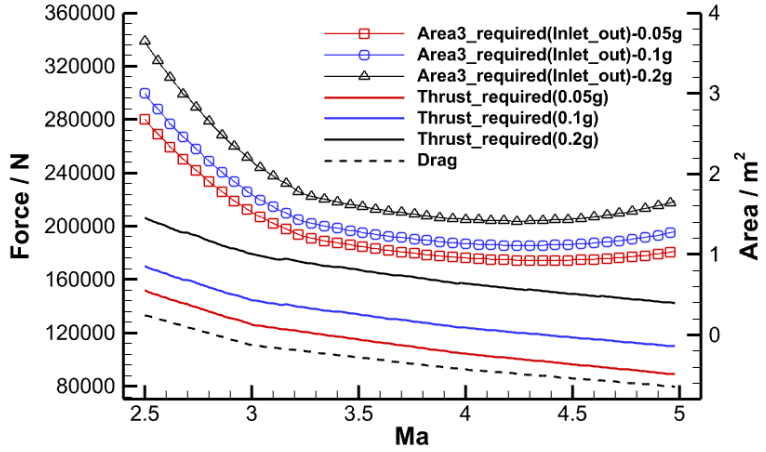

Fig 3. The required thrust of vehicle and A3 of ramjet along the design Ma

Fig 4 displays the acceleration and drag of the aircraft propelled by the ramjet with a selected A3. It shows that the acceleration rise initially, reaching a maximum at Mach 3, and then follows a decline. This trend is influenced by the off-design performance of the ramjet along the trajectory with a constant dynamic pressure. Ideally, a horizontal acceleration line is expected, signifying the most efficient utilization of energy. Therefore, the aim of ramjet design is to flatten the acceleration curve in Fig 4. In fact, the aircraft's acceleration is the cumulative result of thrust, drag, and gravity. As mentioned previously, the cross-sectional area A3 of the ramjet significantly influences thrust and drag characteristics. To enhance the efficiency of propulsion during the climb phase and conserve energy for the cruise phase, an appropriate utilization of gravitational potential energy may be beneficial, which is related to the climb trajectory.

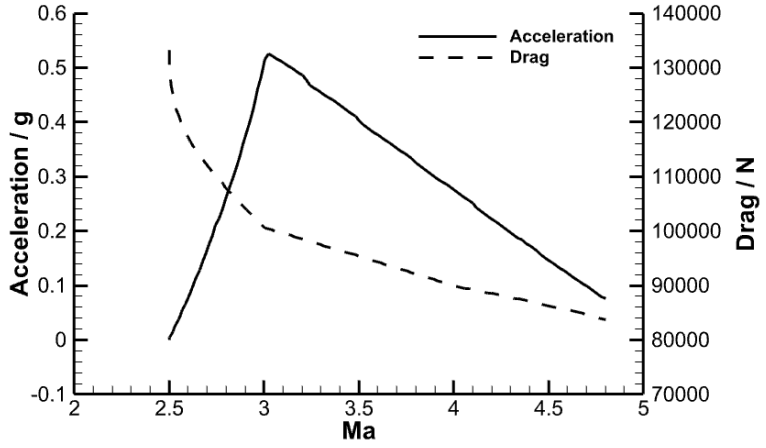

Fig 4. Acceleration and drag of vehicle propelled by ramjet with the selected A3

3. Integrated Analysis Method

3.1. Description of the Aircraft Model

The baseline aircraft is assumed to have an initial weight at Mach 2.5 of 18,130 kg and a wing loading of 105 kg/m^2. The lift and drag coefficients refer to X−43 [8]. For the trajectory optimization in the conceptual design, a point mass model for motion in a vertical plane is usually quite adequate [9]. The equations of motion for this model [10] are given by:

$$\dot{h} = V sin\gamma \tag{1}$$

$$\dot{V} = \frac{T cos\alpha - D}{m} - g sin\gamma \tag{2}$$

$$\dot{\gamma} = \frac{T\sin\alpha + L}{mV} + (\frac{V}{r} - \frac{g}{V})\cos\gamma \tag{3}$$

$$\dot{m} = -\frac{T}{g \cdot Isp} \tag{4}$$

The lift L and drag D are defined as:

$$L = qSC_L(\alpha, Ma) \tag{5}$$

$$D = qSC_D(\alpha, Ma) \tag{6}$$

where q is the flight dynamic pressure and S is the reference area of the vehicle. The lift coefficient C_L and the drag coefficient C_D are the interpolation functions of the attack angle α and the Mach number.

3.2. Description of the Engines Model

This study presents a variable-geometry ramjet engine model. The model represents an axisymmetric ramjet engine, where the axisymmetric inlet center cone can move forward and backward along the axis, and the throat center cone and the exit area of the nozzle can be adjusted. The geometry of the subsonic combustion chamber remains constant. The structural configuration of the engine is depicted in Fig 5. The following sections introduce the models of these three major components. It is worth noting that this study focuses on the size optimization of the fixed cross-section of the combustor in a ramjet engine, but the methods proposed herein can also be applied to other types of engines.

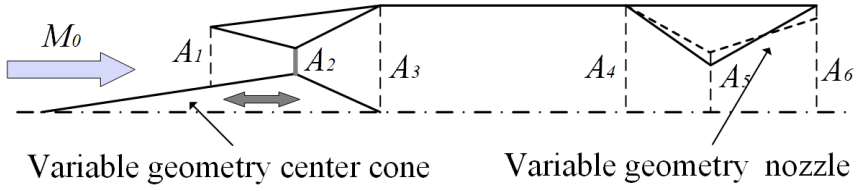

Fig 5. Cross-sections of an axisymmetric ramjet

(1) axisymmetric inlet

This study simplifies the performance of the axisymmetric inlet in subcritical, critical, and supercritical states as follows:

1) In the critical state, shock waves seal the inlet cone top, resulting in no spillage losses.

2) In the subcritical state, shock waves do not seal the inlet cone top, leading to spillage losses.

3) In the supercritical state, shock waves enter the duct without sealing the cone top, resulting in no spillage losses. However, the increased shock wave intensity inside the inlet causes significant disturbances in the shockwave boundary layer and a noticeable decrease in total pressure recovery.

The mentioned performance parameters mainly include the total pressure recovery coefficient σ, capture coefficient φ, and spillage drag coefficient C_x.

Under critical and subcritical states, when the terminating shock wave remains at the throat position, the inlet achieves the maximum total pressure recovery coefficient. The total pressure recovery coefficient is calculated according to the following empirical formula:

$$\sigma_{\max} = 0.97\left(1 - 0.075\left(M_0 - 1\right)^{1.35}\right) \tag{7}$$

When the terminal shock wave resides within the expansion section, the total pressure recovery coefficient of the inlet is simplified as $\sigma = \sigma_{\max} \cdot \sigma_{shock}$, where σ_{shock} represents the loss due to the terminal shock wave, computed using the formula for total pressure loss induced by shock waves.

The calculation of the total pressure recovery coefficient in the supercritical state follows the formula below:

$$\sigma=\sigma_{\max}\cdot(L_{in,r}/L_{in,cr})^2\cdot\sigma_{shock} \tag{8}$$

Where $L_{in,r}$ represents the relative length of the central cone, defined as the length of the protruding central cone over the lip, $L_{in,cr}$ corresponding to the relative length of the central cone in the critical state of the incoming flow Mach number.

In the subcritical state overflow, only the additional drag is considered. The coefficients of additional drag $C_{x,\mathrm{ad}}$ and capture coefficient φ can be calculated by solving through conical shock, with the TM equation employed for computation in this study [11]. The formula for calculating the flow coefficient of a single-stage conical supersonic inlet is as follows:

$$\varphi=\frac{\pi}{4}D_b^2\Big/\frac{\pi}{4}D_0^2=\frac{\sigma\cdot q(M_{ch})\sin(\theta_{ch}-\delta_{ch})}{q(M_0)\sin\theta_{ch}} \tag{9}$$

In the equation, the parameters are referenced to as illustrated in Fig 6, where $\pi D_b^2/4$ and $\pi D_0^2/4$ represent the capture area of the inlet and the free-stream tube area, respectively, while θ_{ch} denotes the position angle of the lip leading edge. Additionally, M_{ch} and δ_{ch} denote the angle of Mach number, velocity with respect to the axis on the OC cone, which can be obtained based on the Mach number of the incoming flow M_0 and the half-cone angle θ_c to solve the conical flow field.

The formula for calculating the drag coefficient is as follows [12]:

$$C_{x,ad}=2\varphi\left(\frac{\lambda_{ch}\cos\delta_{ch}}{\lambda_0}-1\right)+\frac{2}{kM_0^2}\left(\frac{\sigma\pi(\lambda_{ch})}{\pi(\lambda_0)}-1\right) \tag{10}$$

In the equation, apart from the symbols already clarified, λ_0 and λ_{ch} represent the velocity coefficients corresponding to M_0 and M_{ch}, respectively. k represents the specific heat ratio, and $\pi(\lambda)$ is the pressure function in aerodynamics, indicating the ratio of local static pressure to local total pressure, depending on either M or λ.

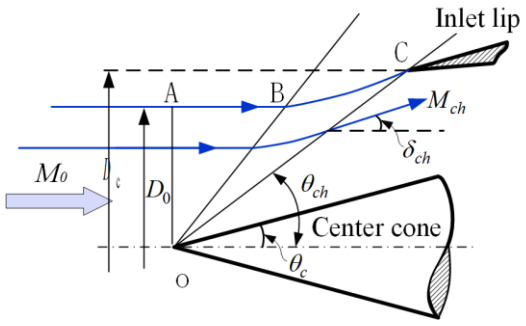

Fig 6. A hybrid inlet with central cone

(2) Combustion Chamber

The calculation of the combustor follows an ideal gas, inviscid, one-dimensional quasi-steady-state model. The fuel-to-air ratio serves as the control variable, considering the effects of combustion efficiency and total pressure recovery coefficient under various inlet conditions [13]. Additionally, there is a constraint on the maximum exhaust temperature of 2200K. Variable specific heat iteration is utilized to calculate outlet parameters, with the detailed process described in reference [14].

$$\eta_c=f(P_3,T_3,V_3,f) \tag{11}$$

$$\sigma_c=g(Ma_3,\tau_{34}) \tag{12}$$

In the equation, P_3, T_3, V_3, Ma_3, f, τ_{34} represent the inlet static pressure, static temperature,

velocity, Mach number, fuel-to-air ratio, and temperature rise ratio of the combustion chamber, respectively.

(3) Convergent/Divergent Nozzle

Addressing the three potential states of completely expanded, under-expanded, and over-expanded in convergent-divergent nozzles (this study temporarily excludes the consideration of subsonic states in the nozzle throat), the thrust coefficients for the outlet of a conical nozzle in the completely expanded and under-expanded states are provided as follows [15]:

$$C_{Fe} = \lambda' \frac{W_a V_6}{P_4^* A_5} + \frac{A_6}{A_5}\left(\frac{P_6}{P_4^*} - \frac{P_0}{P_4^*}\right) \tag{13}$$

In the equation, W_a represents the mass flow, the superscript * denotes total parameters, and X is the expansion factor [15], defined as:

$$\lambda' = (1+\cos\beta)/2 \tag{14}$$

β is the expansion angle of the nozzle divergent section. Addressing the airflow separation phenomenon occurring in the divergent section under over-expansion, the thrust coefficient [15] is expressed as:

$$C_{Fe} = \Gamma\lambda' k\left\{\frac{2}{k-1}\left[1-\left(P_s/P_4^*\right)^{\frac{k-1}{k}}\right]\right\}^{1/2} + \frac{A_s}{A_5}\left(\frac{P_s}{P_4^*} - \frac{P_0}{P_4^*}\right) \tag{15}$$

In the equation, P_s represents the separation pressure, and parameter $\Gamma = \left[2/(k+1)\right]^{(k+1)/(2k-2)}$.

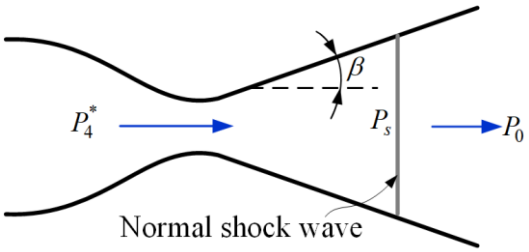

Fig 7. A Laval nozzle in over expanded state

Lastly, the thrust T generated by the ramjet engine equals the difference between the nozzle thrust and the combined effect of incoming momentum and spillage drag [15]. Specific impulse is defined as the ratio of thrust to the fuel consumption W_f per unit time.

$$T = C_{Fe} A_5 P_4^* - W_a V_0 + C_{x,\mathrm{ad}} A_0 \left(0.5\rho_0 V_0^2\right) \tag{16}$$

$$Isp = \frac{T}{W_f g} \tag{17}$$

This study provides information regarding the influence of different combustor cross-sectional sizes on the drag coefficient, which can be found in [16]. It is noteworthy that the component models remain relatively idealized, possibly leading to inadequate consideration of the influence patterns of certain parameters. Nonetheless, the author contends that the general trends of the main parameters are faithfully represented.

3.3. Description of the Trajectory Optimization Method

(1) Optimization Problem

Within the aircraft/engine model, the state parameters consist of altitude h, speed V, climb angle γ,

aircraft weight m, and flight range Range; while the control parameters consist of attack angle α and the fuel throttle opening Thr_T to ensure smooth flight. Based on the aircraft control equations, the trajectory optimization problem can be formulated, incorporating the corresponding cost function and parameter constraints. With the optimization goal set as achieving minimum fuel consumption, the cost functions are formulated as follow:

$$J = zeros\left(size\left(t_f\right)\right) \tag{18}$$

The dynamic pressure q is constrained to be within the range of 10 kPa to 75 kPa. Additional boundary conditions and constraints are detailed in Table 1.

Table 1. Boundary conditions and constraints

Value type	Time	State parameter					Control parameter	
	t/s	h/km	$V/(\mathrm{m/s})$	m/kg	$Range/\mathrm{km}$	γ/deg	α/deg	Thr_T
Initial	0	18	738	30000	0	0	/	/
Terminal	/	26	1500	/	/	/	/	/
Min	10	0	738	10000	0	0	-10	0
Max	300	33.8	1650	30000	/	30	20	1

(2) Gauss Pseudospectral Method

Utilizing the Gauss pseudospectral method (GPM), the optimal control problem described by equations (18) above can be transformed into a continuous Bolza problem. The GPM utilizes Lagrange interpolation polynomials over a set of Legendre points to approximate the system's state variables and control variables, thereby transcribing the continuous optimal control problem into a nonlinear planning problem (NLP). It has been noted that, owing to the equivalence between the Karush-Kuhn-Tucker (KKT) conditions and the discrete first-order necessary conditions, the KKT multipliers of the NLP can be employed to accurately estimate the costate variable at Legendre-Gauss points and boundary points. This study utilizes the general software package GPOPS for solving trajectory optimization problems. For more details about this algorithm, please refer to [17].

4. Results and Discussion

4.1. Analysis and Comparison of Typical Trajectories

This section aims to elucidate the influence of various flight trajectories on the climb performance of the aircraft. It compares the climb phase acceleration and fuel consumption for two typical trajectories, based on the aircraft and engine models detailed in Chapter 3. As depicted in Fig 8, trajectory one entails a climb trajectory along the 33 kPa dynamic pressure line, whereas trajectory two initially maintains level flight before accelerating during the climb. The comparison results of these two typical trajectories are presented in Fig 9. When the aircraft follows the red climb trajectory (horizontal flight before climbing), the flight acceleration initially increases as it does not need to overcome gravitational potential energy. The flight acceleration in the Mach range of the climb phase increases due to the reduced flight altitude, thereby enhancing the thrust force of the engine. It is evident that the acceleration can be adjusted through trajectory optimization. Ultimately, adopting a horizontal flight before climbing trajectory instead of a constant dynamic pressure trajectory resulted in a reduction in fuel consumption during the climb phase by 1163 kg.

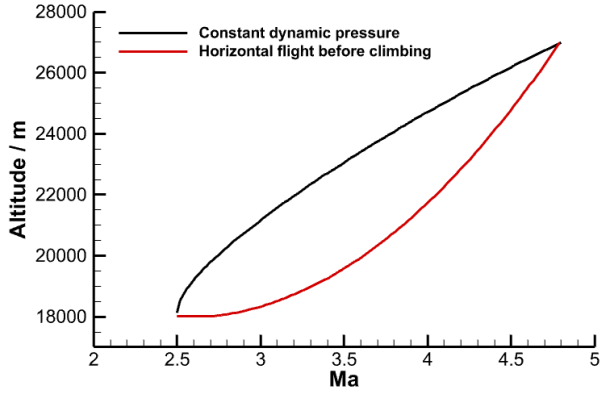

Fig 8. Two kind of climb trajectory

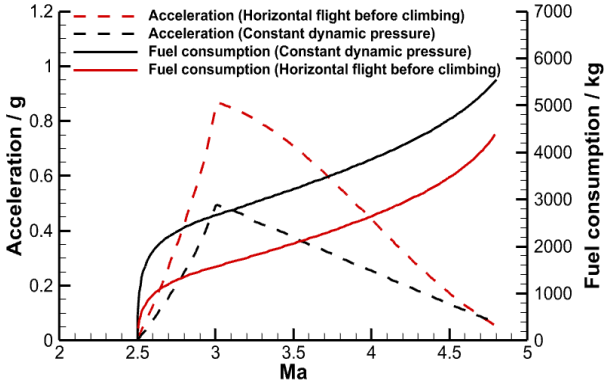

Fig 9. Acceleration and fuel consumption along the two trajectories

4.2. Analysis and Comparison of Optimal Trajectories

In Section 4.1, a comparison was made between the horizontal flight before climbing trajectory and the constant dynamic pressure trajectory, demonstrating that employing rational trajectory optimization can effectively reduce the aircraft's fuel consumption. For an aircraft, an optimal trajectory should exist to further minimize fuel consumption. Therefore, leveraging the integrated analysis method for aircraft/engine outlined in Chapter 3 along with trajectory optimization methods, this section undertakes a comparative analysis of the optimal trajectories and their performance parameters for varying ramjet engine combustor areas. Additionally, size optimization of the ramjet engine combustor is accomplished.

As depicted in Fig 10, the figure illustrates the altitude-Mach number curves for combustor areas of 4/5/6, respectively. In contrast to the horizontal flight trajectory previously discussed in Section 4.1, the optimal trajectories in all three cases extend the range of level flight until accelerating to approximately Mach 3.5 before commencing the climb. The flight trajectories for all three schemes exhibit significant consistency before reaching approximately Mach 4.5. After Mach 4.5, the trajectory for the combustor area of 4 m^2 exhibits a smoother climb trajectory, whereas that of the combustor area of 6 m^2 quickly transitions to a steeper climb after having maintained a lower climb rate for a period. Eventually, all three trajectories converge at the cruise point.

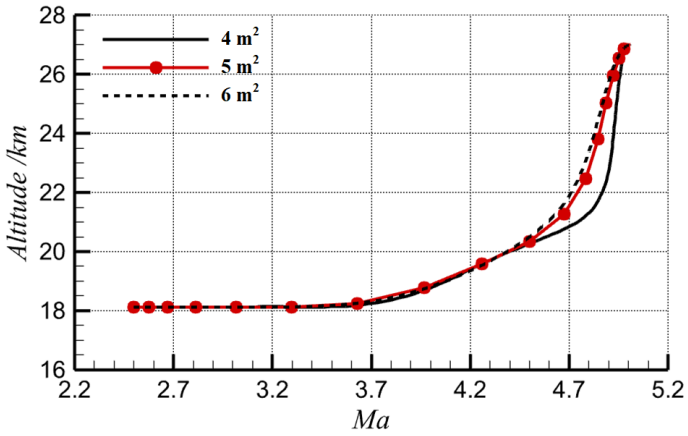

Fig 10. Optimal Trajectories

For comparison of the differences in climb times, Figure 11 illustrates the characteristics of Mach Number-Time for these schemes. The figure demonstrates that with an increase in the combustor area, the engine's thrust is enhanced, resulting in shorter climb times. For the scheme with the 4 m^2 combustor area, due to the lower thrust, the climb time is longest, reaching 172 s because of insufficient acceleration during the rapid climb phase after Mach 4.5. Conversely, the difference in climb times between the schemes with 5 m^2 and 6 m^2 combustor areas is minimal, with climb times of 133 s and 122 s, respectively. This suggests that solely relying on increasing the combustor area for the purpose of reducing climb time is limited due to the increase in frontal drag caused by the larger dimensions.

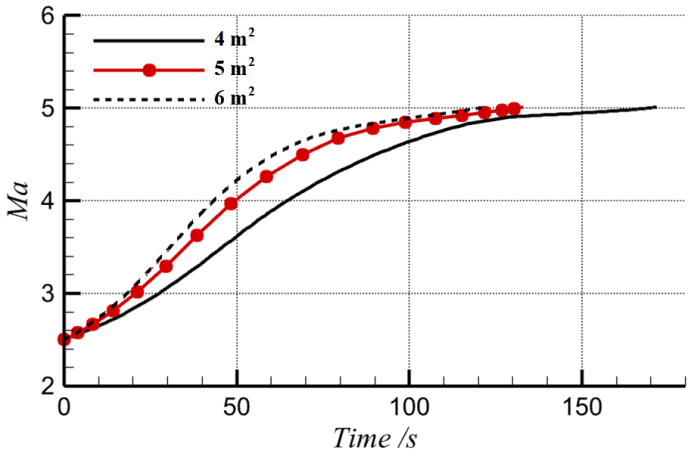

Fig 11. Mach Number-Time Characteristics

Fuel consumption during the climb phase serves as a crucial metric for evaluating aircraft performance. Lower fuel consumption implies that the aircraft can achieve a longer cruising range or carry a greater payload. According to the Fig 12, the scheme with 5 m^2 combustor area exhibits the least fuel consumption, measuring 2733 kg, while the schemes with 4 m^2 and 6 m^2 combustor areas record fuel consumptions of X2931 kg and 2923 kg, respectively. This result suggests that fuel consumption stems from the combined effects of time and drag during the climb phase. Under the combined influence of climb time and drag, there exists an optimal thrust, which corresponds to the optimal size of the combustor cross-section, to minimize fuel consumption during the climb phase.

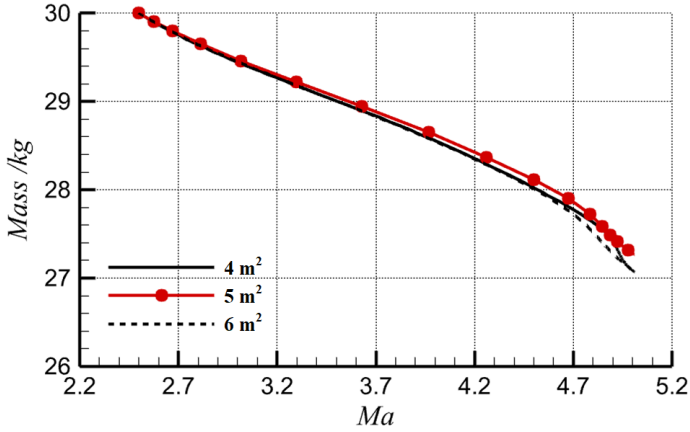

Fig 12. Mass-Mach number Characteristics

Fig 13 depicts the variation of thrust and drag during the climb process in order to further elucidate the influence of different combustor cross-sectional sizes on aircraft performance. With the increase in combustor cross-sectional size, the thrust of the ramjet engine increases linearly. At Mach 3.7, the engine thrust reaches its maximum value. As the aircraft reaches around Mach 4.5 and enters the rapid climb phase, ascending rapidly, the corresponding thrust decreases accordingly. Regarding the drag, with the enlargement of the cross-sectional size and considering the impact of the engine frontal area on drag coefficients, the increase in drag becomes more pronounced. Although the climb time is reduced, the combination of these factors results in higher fuel consumption for 6 m^2 scheme compared to 5 m^2 scheme. Additional analysis will be provided in subsequent related studies.

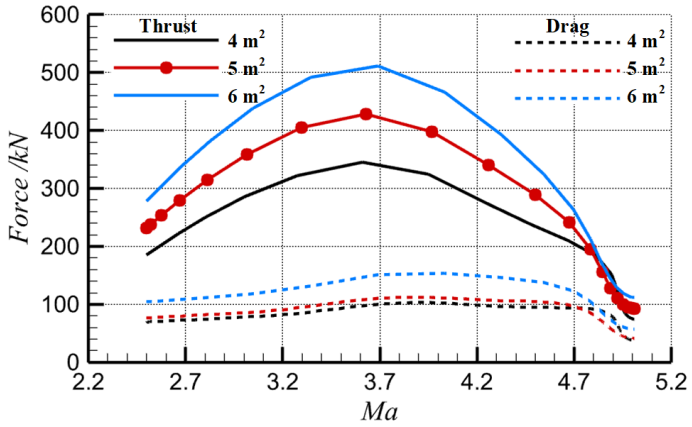

Fig 13. Thrust and Drag Characteristics

For further illustration of the variation of aircraft fuel consumption with respect to combustor cross-sectional size, Fig 14 depicts the fuel consumption during the climb phase for different combustor areas. According to the figure, it is observed that as the combustor cross-sectional size increases, fuel consumption initially decreases and then increases, reaching a minimum value of 2723 kg at a combustion chamber cross-sectional size of 5.2 m^2. In comparison to 4 m^2 and 6 m^2 schemes, fuel consumption decreases by 208 kg (7.1%) and 200 kg (6.8%), respectively. Although adopting different aircraft and engine parameters may lead to variations in results, the general trend remains consistent.

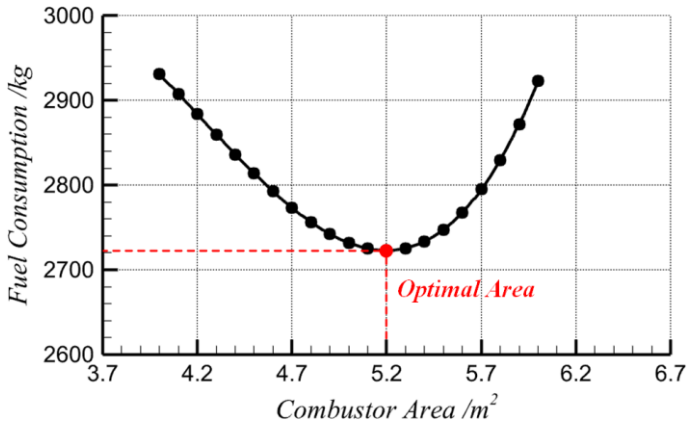

Fig 14. Sizing Optimization of Combustor

5. Conclusion

This study establishes an analysis method for aircraft/engine integration of a ramjet engine and optimizes the sizing of the fixed cross-section of the combustor in a ramjet engine. The primary findings are as follows:

1. In wide-speed-range hypersonic aircraft, the climb phase is also important in terms of aircraft performance, and the design of the aircraft needs to consider both on-design and off-design conditions.
2. Optimizing trajectories can reduce fuel consumption during the climb phase. For example, in the climb phase, compared to a trajectory with constant dynamic pressure, adopting the horizontal flight before climbing trajectory results in fuel consumption reduction by 1163 kg (21%).
3. An optimal value exists for the cross-sectional size of the ramjet combustor that minimizes fuel consumption during the climb phase. Under the optimal trajectory, with the combustor area at 5.2 m^2, fuel consumption is reduced by 208 kg (7.1%) compared to 4 m^2 and 200 kg (6.8%) compared to 6 m^2.
4. The focus of this study is on introducing modeling methods and cross-sectional size optimization methods for the ramjet combustor. These results reflect only the trends under certain assumptions. Employing more accurate and precise models could further increase the confidence in the analysis

results.

References

1. Fry R S.: A Century of Ramjet Propulsion Technology Evolution. Journal of Propulsion and Power, 2004, 20(1): 27-58.
2. Huang W, Wang Z G, Jin L, et al.: Effect of Cavity Location on Combustion Flow Field of Integrated Hypersonic Vehicle in Near Space. Journal of Visualization, 2011, 14(4): 339-351.
3. Heiser W H, Pratt D T.: Hypersonic Airbreathing Propulsion. AIAA, 1994.
4. Minard J P, Hallais M, Falempin F.: Low cost ramjet technology for tactical missile application, AIAA 2002 -3765. USA: AIAA, 2002.
5. Curran E T.: Scramjet Engines: the First Forty Years. Journal of Propulsion and Power, 2001, 17(6): 1138-1148.
6. Paul L. Moses, Vincent L. Rausch, Luat T. Nguyen, Jeryl R. Hill.: NASA hypersonic fight demonstrators—overview, status, and future plans. Acta Astronautica, 2004 (55) 619-630.
7. Waltrup P J, White M E, Zarlingo F, et al. History of US Navy ramjet, Scramjet, and Mixed-Cycle Propulsion Development. Journal of Propulsion and Power, 2002, 18(1): 14-27.
8. Brock M.A. Performance Study of Two-Stage-To-Orbit Reusable Launch Vehicle Propulsion Alternatives. Air Force Institute of Technology. Master's Thesis, AIR Force Institute of Technology, Wright-Patterson AFB, OH, USA, 2004.
9. Bryson J.A.E., Desai M.N., Hoffman W.C. Energy-state approximation in performance optimization of supersonic aircraft. J. Aircr. 1969, 6, 481–488.
10. Parker J.T., Bolender M.A; Doman D.B. Control-oriented modeling of an air-breathing hypersonic vehicle. J. Guid. Control Dyn. 2007, 30, 856–869.
11. Zucrow M J, Hoffman J D. Gas dynamics. Volume 2 - Multidimensional flow. New York, John Wiley & Sons Inc.p, 1977.
12. BARRY F W. An Explicit Formula for Additive Drag of a Supersonic Conical Inlet. Journal of Aircraft, 1971, 8(4):279-280.
13. Reynolds T W, Graves C C, Childs J H. Relation of Turbojet and Ramjet Combustion Efficiency to Second-Order Reaction Kinetics and Fundamental Flame Speed. National Advisory Committee for Aeronautics-Report 1334.
14. Lian, X. C. Principles of Aero Engines. Xi'an: Northwestern Polytechnical University Press, 2005. (in Chinese)
15. The Johns Hopkins University Applied Physics Laboratory. Ramjet Engine Technology. Volume I. Beijing: National Defense Industry Press, 1980. (in Chinese)
16. Li, Y., Jiang G.T., Ch X.Y., Wang J. Research on TBCC Engine Size Selection and Ascent Strategy of Combined-Cycle Aircraft. J. Astronaut. 2018, 39, 17–26.
17. C.L. Darby, W.W. Hager, A.V. Rao. An hp-adaptive pseudospectral method for solving optimal control problems, Optim. Control. Appl. Methods 32 (2011) 476–502.